CRYSTAL GROWTH & DESIGN

pubs.acs.org/crystal

Article

Kinetically Limited Molecular Beam Epitaxy of $B_xGa_{1-x}As$ Alloys

Kyle M. McNicholas, Rasha H. El-Jaroudi, and Seth R. Bank*

Cite This: https://doi.org/10.1021/acs.cgd.1c00291

Read Online

ACCESS | Metrics & More | Article Recommendations | Supporting Information

ABSTRACT: The small lattice constants of the boron pnictides present exciting new opportunities for strain engineering and lattice-matching of III−V semiconductor heterostructures. However, the challenging synthesis of boron-containing III−V alloys has limited the achievable B concentrations to only dilute amounts, hindering both the ultimate application of these materials and experimental investigations of their electronic and optical properties. Using $B_xGa_{1-x}As$ on GaAs and GaP substrates as prototype, we demonstrate a highly kinetically limited molecular beam epitaxy growth regime capable of achieving high substitutional incorporation of boron. By combining the effects of low growth temperature and surfactant-mediated epitaxy with the high boron fluxes accessible with electron-beam evaporation, we achieved substitutional boron incorporation up to a 15% mole fraction, nearly double that of previous reports.

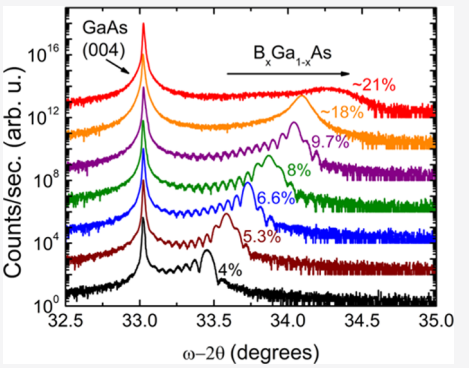

INTRODUCTION

The boron pnictides (B-V) remain as some of the least explored III−V compound semiconductors. The lattice constants of these zinc-blende compounds are significantly smaller than those of the conventional zinc-blende III−V semiconductors, with values ranging from 4.55 Å for BP[1] to 5.1 Å for BSb.[2] Owing to the challenges in pseudomorphic heterostructure growth arising from compressive mismatch of many III−V materials with commercially available substrates, the B-V compounds have received attention for their potential application in heterostructure strain engineering. To date, dilute-boride alloys have been shown to effectively reduce compressive strain through alloying with InGaAs[3,4] and GaAsBi[5] for solar cell devices and InGaAs[6,7] for quantum well optical sources on GaAs and to compensate highly compressively strained quantum well optical sources on GaP-on-Si virtual substrates.[8,9] In analogy to dilute-nitride III−V alloys, the large tensile mismatch of B-V compounds with conventional substrates provides new avenues for compensation of compressively strained layers using III−V alloys incorporating relatively small amounts of B. However, despite predictions of increased solid solubility of B over N in analogous highly mismatched nitride alloys,[10] reports of high-quality $B_xGa_{1-x}As$ alloys have thus far remained limited to dilute concentrations, limiting their ultimate application for strain engineering. For example, $B_xGa_{1-x}As$ is particularly enticing for potential monolithic integration of direct-gap III−V materials with Si. However, the incorporation of ∼ 25% B is necessary for lattice-matched epitaxial growth of $B_xGa_{1-x}As$ on Si.

Nonsubstitutional incorporation of B in these alloys has proven to be a significant challenge as the B concentration is increased beyond dilute concentrations, with reports of antisite incorporation,[11,12] interstitial incorporation,[13,14] and phase separation of boron[15,16] inhibiting the growth of high-quality materials. As with other highly mismatched alloys, optimization of growth conditions has proven critical to increasing the substitutional incorporation of B. In materials grown with molecular beam epitaxy (MBE), fast growth rate[17] and reduced substrate temperatures,[13,14] in concert with large V:III flux ratios[13] and surfactant-mediated epitaxy,[14] have been shown to promote substitutional incorporation of B. Similarly, low growth temperatures,[15,16,18] high V:III precursor ratios,[15] and optimized precursor chemistry[19] have enabled the highest concentrations of B in metal-organic chemical vapor deposition (MOCVD)-grown $B_xGa_{1-x}As$. Despite these optimizations, substitutional B concentrations in BGaAs reported in the literature remain limited to less than ∼8% in both MBE-[13] and MOCVD[18]-grown materials. The inability to incorporate nondilute concentrations of boron places a practical limit on the use of boron for strain engineering applications. To this end, we demonstrate an optimized highly kinetically limited MBE growth approach that enables an ∼2× increase in substitutional boron incorporation over previously reported values, expanding the applicability of these alloys for strain engineering.

Received: March 14, 2021
Revised: September 15, 2021

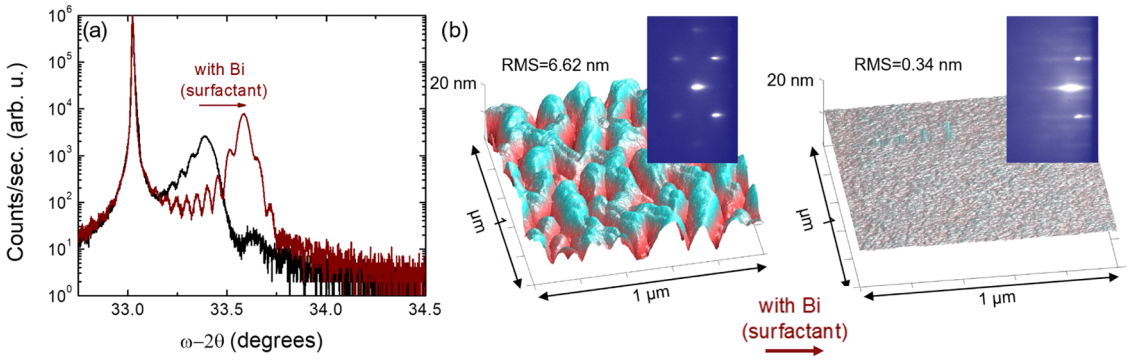

Figure 1. (a) HR-XRD ω-2θ scans of 100 nm $B_{0.05}Ga_{0.95}As$/GaAs heterostructures grown with (red) and without (black) Bi-surfactant flux. (b) AFM surface morphology measurements and (inset) RHEED diffraction patterns from the samples shown in panel (a).

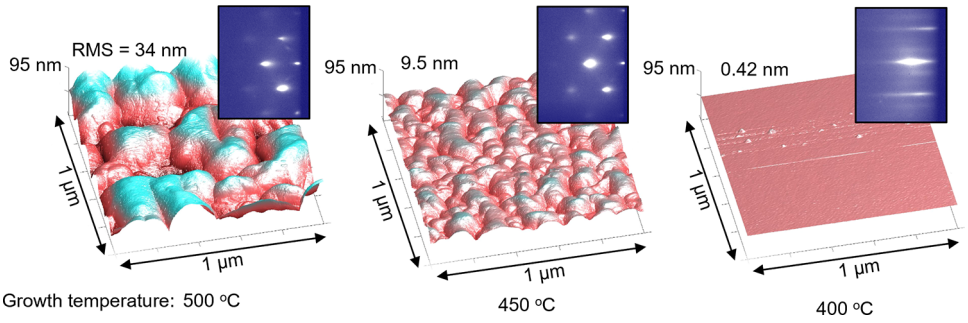

Figure 2. AFM surface morphology measurements and (inset) RHEED diffraction patterns from $B_{0.10}Ga_{0.90}As$/GaAs heterostructures grown at 500 °C (left), 450 °C (middle), and 400 °C (right).

EXPERIMENTS AND DISCUSSION

Our dilute-boride growth approach builds on the work of Groenert et al.[13] and Ptak et al.[14] In particular, Groenert et al. demonstrated that interstitial B incorporation increases in MBE-grown BGaAs at substrate growth temperatures exceeding 500 °C.[13] Ptak et al. expanded on this work by investigating surfactant-mediated epitaxy of BGaAs and showed that the introduction of a Bi-surfactant flux during $B_xGa_{1-x}As$ MBE growth can reduce interstitial B incorporation in dilute (~1% B) $B_xGa_{1-x}As$ films at substrate growth temperatures exceeding 500 °C.[14]

We first addressed the challenging elemental B flux requirements necessary for MBE growth of high B-content alloys. Boron has the lowest vapor pressure of the group-III elements, necessitating deposition sources capable of prolonged operations above 1800 °C to achieve even moderate B fluxes, prohibiting the use of conventional PBN crucibles, which thermally decompose above ~1400 °C. The choice of a deposition source is further complicated by the formation of B-refractory eutectics,[20] limiting the use of conventional refractory metal high-temperature effusion cell sources. Our initial growth experiments utilized a high-temperature effusion cell with a tungsten crucible, which exhibited severe structural degradation after several hours of operations at 1850 °C. Pyrolytic graphite crucible liners are often used to mitigate such eutectic reactions[12] but are critically limited by the unintentional codeposition of electrically active C. To avoid the limitations of conventional effusion cell sources, we employed an electron-beam evaporation source for B deposition. The water-cooled evaporator hearth effectively suppresses B eutectic reactions with the refractory metal hearth liner while simultaneously providing a higher local evaporant temperature, enabling B fluxes >4× larger than those accessible with a conventional high-temperature effusion cell and subsequently the growth of nondilute BGaAs alloys at typical MBE growth rates of ~0.5−1 μm/h.

We then investigated the impact of surfactant-mediated epitaxy in nondilute BGaAs alloys by growing nominally identical 100 nm $B_{0.05}Ga_{0.95}As$ films at a growth temperature of 400 °C with and without a Bi-surfactant overpressure of 5×10^{-8} Torr. *In situ* reflection high-energy electron diffraction (RHEED) patterns, monitored during growth to provide a qualitative assessment of surface morphology, showed significant improvement with the addition of a Bi-surfactant flux. As shown in Figure 1 (inset), the sample grown without Bi exhibited a spotty (1 × 1) reconstruction, consistent with the roughening of the epi surface during growth, while the sample grown with a Bi-surfactant flux exhibited a streaky (1 × 3) reconstruction, in agreement with findings of Ptak et al.[14] and consistent with reports of Bi-terminated GaAs surfaces.[21,22] Atomic force microscopy (AFM) was used to quantify changes in the surface morphology and showed good correlation with the observed RHEED diffraction patterns. Growth without Bi resulted in a rough, irregular morphology, with a root-mean-square (RMS) roughness of 6.2 nm. The addition of Bi resulted in a smooth surface morphology, reducing the RMS roughness to 0.34 nm, comparable to that of homoepitaxial GaAs.

The changes in surface morphology also correlated to changes in bulk structural quality, as measured using high-resolution X-ray diffraction (HR-XRD) ω-2θ measurements. Growth without Bi resulted in a broad BGaAs diffraction peak with low-intensity finite-thickness fringes, indicating interfacial/structural disorder within the BGaAs epilayer. The addition of a Bi-surfactant flux significantly improved the bulk structural quality, simultaneously narrowing the BGaAs

https://doi.org/10.1021/acs.cgd.1c00291
Cryst. Growth Des. XXXX, XXX, XXX−XXX

layer diffraction peak and producing distinct finite-thickness fringes, consistent with increased crystalline quality. The improvement in structural quality was accompanied by a shift of the BGaAs diffraction peak to larger diffraction angles, indicating an increase in substitutional B incorporation with the use of a Bi-surfactant flux. In contrast to the findings of Ptak et al. at elevated temperatures,[14] we observed no clear dependence of substitutional B incorporation on Bi-surfactant flux, suggesting that the Bi flux does not need to be tightly controlled for unity substitutional B incorporation at reduced growth temperatures.

To assess the impact of substrate temperature on substitutional B incorporation in nondilute BGaAs alloys grown with surfactant-mediated epitaxy, we grew 100 nm $B_{0.10}Ga_{0.90}As$ films while maintaining a Bi overpressure of 5×10^{-8} Torr and varied the substrate temperature from 400 to 500 °C in 50 °C steps across a series of samples. As shown in Figure 2, changes in the growth substrate temperatures produced significant changes in the surface morphology of the BGaAs epilayer. Samples grown at 500 °C exhibited an extremely rough, irregular surface morphology, with an RMS roughness of 34 nm measured using AFM. The corresponding (1 × 1) RHEED pattern consisted of spotty, chevron-like features, consistent with the rough AFM surface morphology measurements. Decreasing the substrate temperature to 450 °C resulted in a lower AFM RMS roughness of 9.5 nm, and reducing the substrate temperature to 400 °C restored the streaky (1 × 3) RHEED reconstruction and reduced the measured RMS roughness still further to 0.42 nm. As shown in Figure 3, the

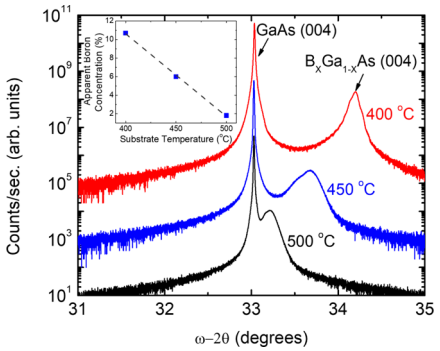

Figure 3. HR-XRD ω-2θ diffraction measurements from 100 nm $B_{0.10}Ga_{0.90}As$/GaAs heterostructures grown at 500 °C (black), 450 °C (blue), and 400 °C (red) and (inset) estimated substitutional B incorporation as a function of growth temperature; corresponding AFM surface morphology and RHEED diffraction patterns are shown in Figure 2.

changes in morphology correlated with a significant change in the apparent B concentration, as estimated from the diffraction angle of the BGaAs layer peak in HR-XRD ω-2θ measurements. The apparent B concentration decreased linearly as the substrate temperature was increased, ranging from ∼10.5% at 400 °C to ∼1.5% at 500 °C (Figure 3, inset).

Previous reports of adatom surface diffusion as a function of epilayer growth rate in GaAs MBE heteroepitaxy indicate a linear decrease in surface diffusion length with increasing epilayer growth rate,[23] indicating that the fast growth rates enabled by e-beam deposition of B reduce surface adatom diffusion lengths. Likewise, following the Arrhenius dependence of surface adatom diffusion on the substrate temperature,[24] the diffusion length of surface B adatoms is increasingly limited as the substrate temperature is reduced during BGaAs growth. Finally, the introduction of surfactant flux, originally employed to inhibit 3D growth of GeSi on Si,[25] and later extended to III−V strained layer heterostructures,[26] is thought to reduce adatom surface diffusion lengths by enhancing the incorporation of surface adatoms through preferential exchange reactions.[27−29] Substitutional incorporation of Bi is minimized under MBE growth conditions with large As/Bi flux ratios or at substrate temperatures >350 °C,[30] making it an ideal surfactant in III−V epitaxy, where it has been shown to inhibit 3D growth in highly strained InGaAs layers[31] and increase the incorporation of N in dilute-nitride alloys.[32,33] Accordingly, combining the elevated growth rate enabled by an e-beam B source with a low substrate growth temperature and the use of a Bi-surfactant flux defines a highly kinetically limited growth regime, in which the B surface adatom diffusion length is reduced significantly. The observed decrease in surface roughness and the corresponding increase in apparent B concentration with the reduction of substrate temperature and introduction of Bi-surfactant suggest a preference for elemental boron to self-segregate to the epilayer surface during MBE growth, consistent with previous reports of surface B accumulation in MOCVD-grown BGaAs.[16] This surface-segregation phenomena may arise from the formation of thermodynamically stable boron subpnictide crystal phases ($B_{12}As_2$)[34,35] or through the formation of B−B clusters,[15,36,37] which should be reduced by minimizing the interaction of B surface adatoms by kinetically limiting their surface diffusion length.

To access the higher B concentrations necessary for flexible strain engineering, we grew a series of 100 nm BGaAs films, increasing the supplied B fluxes while maintaining constant Ga and Bi fluxes, As:III flux ratios, and a growth substrate temperature of 400 °C. As the B concentration was increased, the streaky (1 × 3) reconstruction and corresponding monolayer-scale RMS roughness in AFM were maintained in all samples. HR-XRD ω-2θ measurements of the samples incorporating <10% B (Figure 4) showed narrow diffraction peaks with full width at half-maximum (FWHM) values ranging from 0.0496 to 0.0556° and pronounced finite-thickness fringes, indicating high structural quality. XRD reciprocal space maps about the (224) diffraction peak (shown in Supporting Information Figure S1a) confirmed coherent nucleation of the BGaAs layers incorporating up to 9.7% B, enabling straightforward calculation of the B concentration in epilayers exhibiting high structural quality. Repeated growths of BGaAs films incorporating <10% B exhibited comparable structural quality, as measured using HR-XRD, demonstrating high repeatability using this optimized growth approach. Estimating the B concentration (∝ B flux) from the $B_xGa_{1-x}As$ HR-XRD diffraction peak from a series of samples grown with varying e-beam power across a single growth day, we observed the expected Arrhenius dependence of B concentration on the B e-beam evaporator power (∝ temperature), suggesting near-unity substitutional incorporation of B. The observed Arrhenius relationship between the B concentration and e-beam evaporator power was highly repeatable across multiple growth days, providing an alternative to conventional beam equivalent pressure measurements for B flux calibrations, which are complicated by the formation of B-W eutectics.

Films incorporating >10% B exhibited signs of structural degradation in HR-XRD, as indicated by the absence of finite-

https://doi.org/10.1021/acs.cgd.1c00291
Cryst. Growth Des. XXXX, XXX, XXX−XXX

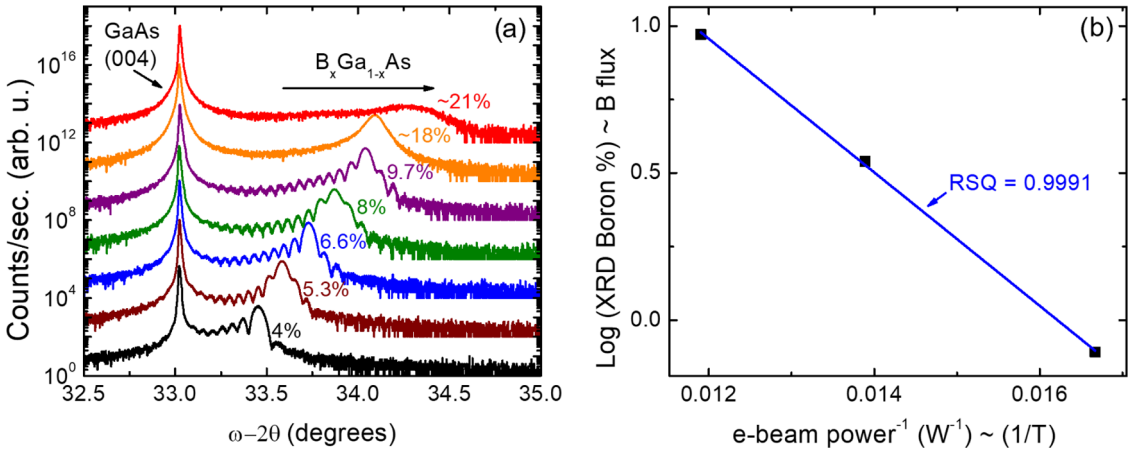

Figure 4. (a) HR-XRD ω-2θ diffraction measurements from 100 nm $B_xGa_{1-x}A$/GaAs heterostructures grown under optimized growth conditions; excellent structural quality was maintained in films incorporating up to ~10% B. (b) HR-XRD B concentration as a function of the inverse of the B e-beam evaporator power.

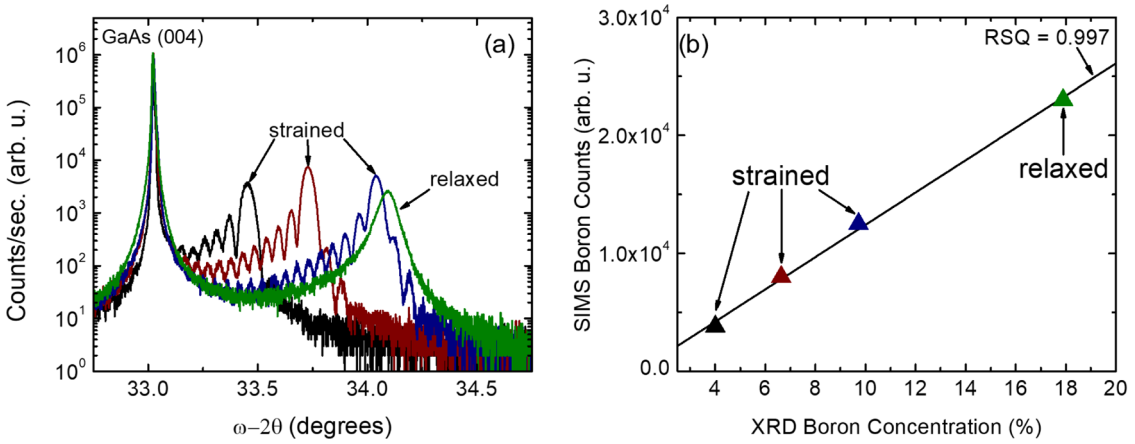

Figure 5. (a) HR-XRD ω-2θ diffraction measurements from 100 nm $B_xGa_{1-x}A$/GaAs heterostructures with B concentrations spanning coherent (black, red, blue) and structurally degraded (green) compositions. (b) B secondary ion yield in SIMS versus apparent B concentration determined from the HR-XRD measurements shown in panel (a).

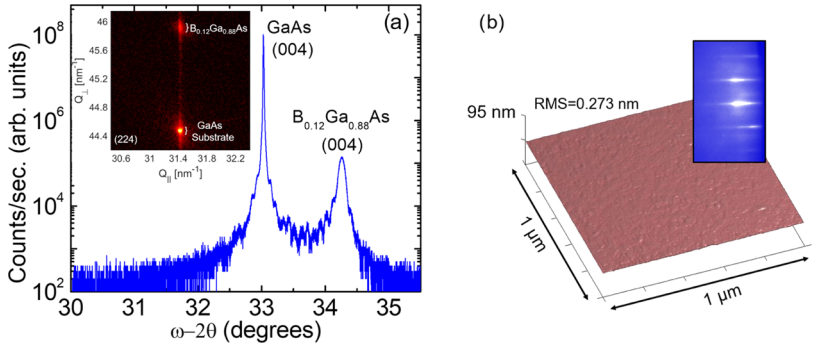

Figure 6. (a) HR-XRD ω-2θ diffraction measurement and (inset) XRD reciprocal space map from 50 nm $B_{0.12}Ga_{0.88}As$/GaAs heterostructures. (b) AFM surface morphology measurements showing atomic-level RMS surface roughness and (inset) RHEED diffraction patterns from $B_{0.12}Ga_{0.88}As$/GaAs heterostructures.

thickness fringes and an increase in the BGaAs layer diffraction peak FWHM to 0.0775° at ~18% B and 0.2147° at ~21% B, as shown in Figure 4. Following the work of Groenert et al., who noted a significant disparity between $B_xGa_{1-x}As$ B concentrations measured using secondary ion mass spectrometry (SIMS) and XRD under unoptimized growth conditions,[13] we probed the origin of this structural degradation by comparing the SIMS B ion yield to the B concentrations calculated from the $B_xGa_{1-x}As$ diffraction peak position in HR-XRD. Assuming complete relaxation of the structurally degraded $B_xGa_{1-x}As$ sample, we observed a linear relationship between the SIMS B ion yield and the concentrations estimated from HR-XRD measurements (Figure 5), consistent with near-unity substitu-

https://doi.org/10.1021/acs.cgd.1c00291
Cryst. Growth Des. XXXX, XXX, XXX−XXX

tional B incorporation, and suggesting an alternative source of structural degradation.

As the $B_xGa_{1-x}As$ B concentration was increased beyond 10%, the tensile lattice mismatch of the $B_xGa_{1-x}As$ epilayer with the GaAs substrate increased to >1.5%. The tensile mismatch corresponds to a critical thickness of <8 nm before the onset of strain relaxation, as estimated using the model of Matthews and Blakeslee.[38] Additionally, crack-like features were observed in dark-field microscope images of the structurally degraded samples at elevated B concentrations, consistent with reports of grooves/cracks in relaxed tensile InGaAs/InP heterostructures.[39] This suggests that structural degradation observed in 100 nm $B_xGa_{1-x}As$/GaAs heterostructures incorporating >10% B was simply due to strain relaxation. Indeed, decreasing the sample thickness to 50 nm increased the maximum achievable B concentration to 12% before the onset of structural degradation. As shown in Figure 6, the 50 nm $B_{0.12}Ga_{0.88}As$ film exhibited excellent structural quality in HR-XRD while maintaining planar surface morphology. Further increasing the B concentration reduced the estimated critical thickness to <5 nm, necessitating growth on substrates with lattice constants smaller than GaAs. GaP was an ideal choice to further probe the range of accessible B concentrations as it provides a smaller lattice constant for $B_xGa_{1-x}As$ alloys <23% B. To this end, we transitioned our optimized growth approach to GaP substrates, first growing a 20 nm GaP buffer followed by a 50 nm $B_xGa_{1-x}As$ film while maintaining the Ga and Bi fluxes, As:III flux ratios, and 400 °C substrate temperature used in the growth on GaAs. While the Matthews−Blakeslee critical thickness considers only the absolute value of the epilayer lattice mismatch, studies of relaxation in tensile and compressive epilayers have shown that the relaxation mechanisms change as the sign of the mismatch changes, with relaxed tensile layers exhibiting grooved or cracked morphology and relaxed compressive layers exhibiting ridge or island morphology.[40] Additionally, studies of relaxation in tensile and compressive InGaAs/InP heterostructures have shown an increase in critical thickness in tensile layers over comparable strained compressive layers.[39] Accordingly, we targeted >14% B concentrations for our initial growths on GaP so that the absolute value of the lattice mismatch with GaP was <75% of the maximum mismatch observed in coherent samples grown on GaAs. HR-XRD measurements of $B_xGa_{1-x}As$ films incorporating 15% B on GaP (Figures 7 and S2) showed structural quality comparable to that of films incorporating <10% B on GaAs, further suggesting that the ultimate B concentrations achievable in $B_xGa_{1-x}As$ alloys grown on GaAs are limited by strain relaxation, rather than solubility. These initial results also highlight the future potential for heterostructure strain engineering using III−V alloys with nondilute B concentrations.

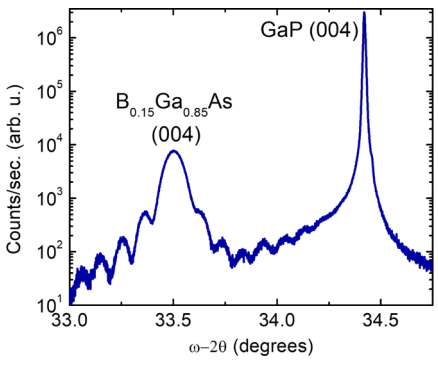

Figure 7. HR-XRD ω-2θ diffraction measurement from a 50 nm $B_{0.15}Ga_{0.85}As$/GaP heterostructure.

CONCLUSIONS

In conclusion, we have developed an optimized MBE growth approach for BGaAs alloys to achieve elevated levels of substitutional B incorporation. Utilizing an electron-beam evaporation source for B deposition, we achieved B fluxes sufficient for the growth of BGaAs at elevated B concentrations and typical MBE growth rates. Consistent with previous reports of increased substitutional B incorporation with increased growth rates,[17] our findings indicate that the increased growth rate accessible with larger elemental B fluxes is critical to the realization of high-quality $B_xGa_{1-x}As$ alloys incorporating nondilute concentrations of B. Combining elevated boron fluxes with low substrate temperatures and surfactant-mediated epitaxy, which had previously been shown to improve substitutional B incorporation in dilute $B_xGa_{1-x}As$ alloys,[13,14] yielded a highly kinetically limited growth window capable of near-unity substitutional B concentrations up to 15% in BGaAs, nearly double the highest reported literature values. This enabled coherent growth of BGaAs on GaP substrates for the first time and, owing to the near-lattice-match between GaP and silicon, suggests the possibility of coherent growth of direct-band-gap B-III−V alloys on silicon.

EXPERIMENTAL METHODS

The samples in this study were grown using solid-source molecular beam epitaxy on the exact (100)-oriented semi-insulating GaAs and GaP substrates. The transparent GaP substrates were indium-bonded to Si carrier wafers prior to epitaxial growth to ensure uniform heating from the substrate heater. Dual-filament SUMO effusion cells were used for the deposition of Ga and Bi, a Mark IV-valved As cracker source operated at 850 °C was used to supply dimeric As_2, a single zone effusion cell with a Ga collecting baffle inset was used to supply elemental P through thermal decomposition of the GaP source material, and an MBE Komponenten electron-beam evaporation source was used for B deposition. The substrate temperature during growth was monitored using optical pyrometry, with a wavelength response centered at 900 nm to provide accurate measurements at low temperatures. The Ga flux was maintained at a value of 3.8×10^{14} atoms cm^{-2} s^{-1}, corresponding to a GaAs growth rate of 0.63 μm/h (1.75 Å/s), a GaP growth rate of 0.57 μm/h (1.57 Å/s), and BGaAs growth rates of ∼0.65−0.68 μm/h (1.8−1.9 Å/s). The group-V/Ga beam equivalent pressure ratio was maintained at ∼18:1, corresponding to a group-V/Ga flux ratio of approximately 3.5:1. Ga fluxes were measured using conventional group-III limited RHEED oscillations, and group-V fluxes were approximated by modifying the method of Svensson et al.[41] to measure the transition from group-III to group-V limited RHEED oscillations and subsequently the group-V BEP corresponding to a 1:1 incorporation of III and V fluxes. HR-XRD measurements were performed using a Rigaku SmartLab diffractometer equipped with a 9 kW Cu anode. Estimates of the BGaAs concentrations from coupled ω-2θ scans were performed with dynamic X-ray scattering simulations using BGaAs elastic constants interpolated between known values for GaAs from the International Crystal Structure Database, as well as predicted values for BAs from first principles.[42] AFM measurements were performed with a Veeco Dimension 3100 AFM. SIMS measurements were performed in the negative-ion collection mode using an IONTOF TOF-SIMS 5 with a Bi_3^+ primary ion beam.

https://doi.org/10.1021/acs.cgd.1c00291
Cryst. Growth Des. XXXX, XXX, XXX−XXX

■ ASSOCIATED CONTENT

Supporting Information

The Supporting Information is available free of charge at https://pubs.acs.org/doi/10.1021/acs.cgd.1c00291.

High-resolution X-ray diffraction reciprocal space maps from coherent and structurally degraded $B_xGa_{1-x}As$/GaAs heterostructures and coherent $B_{0.15}Ga_{0.85}As$/GaP heterostructures (PDF)

■ AUTHOR INFORMATION

Corresponding Author

Seth R. Bank − *Microelectronics Research Center, Electrical and Computer Engineering Department, The University of Texas at Austin, Austin, Texas 78758, United States;* orcid.org/0000-0002-5682-0126; Email: sbank@ece.utexas.edu

Authors

Kyle M. McNicholas − *Microelectronics Research Center, Electrical and Computer Engineering Department, The University of Texas at Austin, Austin, Texas 78758, United States;* orcid.org/0000-0002-2426-2027

Rasha H. El-Jaroudi − *Microelectronics Research Center, Electrical and Computer Engineering Department, The University of Texas at Austin, Austin, Texas 78758, United States*

Complete contact information is available at: https://pubs.acs.org/10.1021/acs.cgd.1c00291

Author Contributions

The manuscript was written through contributions of all authors. All authors have given approval to the final version of the manuscript.

Funding

This work was supported by the National Science Foundation under EECS-1933836 and EECS-1838984.

Notes

The authors declare no competing financial interest.

■ REFERENCES

(1) Popper, P.; Ingles, T. A. Boron Phosphide, a III−V Compound of Zinc-Blende Structure. *Nature* **1957**, *179*, 1075.

(2) Das, S.; Bhunia, R.; Hussain, S.; Bhar, R.; Chakraborty, B.; Pal, A. Synthesis and characterization of boron antimonide films by pulsed laser deposition technique. *Appl. Surf. Sci.* **2015**, *353*, 439−448.

(3) Geisz, J.; Friedman, D.; Kurtz, S. BGaInAs solar cells lattice-matched to GaAs. In *Conference Record of the Twenty-Eighth IEEE Photovoltaic Specialists Conference*, 2000.

(4) Leibiger, G.; Krahmer, C.; Bauer, J.; Herrnberger, H.; Gottschalch, V. Solar cells with (BGaIn)As and (InGa)(NAs) as absorption layers. *J. Cryst. Growth* **2004**, *272*, 732−738.

(5) Beaton, D. A.; Ptak, A.; Alberi, K.; Mascarenhas, A. Quaternary bismide alloy ByGa1-yAs1-xBix lattice matched to GaAs. *J. Cryst. Growth* **2012**, *351*, 37−40.

(6) Gottschalch, V.; Leibiger, G.; Benndorf, G. MOVPE Growth of BxGa1-xAs, BxGa1-X-yInyAs, and BxAl1-xAs Alloys on (001) GaAs. *J. Cryst. Growth* **2003**, *248*, 468−473.

(7) El-Jaroudi, R. H.; McNicholas, K. M.; Briggs, A. F.; Sifferman, S. D.; Nordin, L.; Bank, S. R. Room-Temperature Photoluminescence and Electroluminescence of 1.3-Mm-Range BGaInAs Quantum Wells on GaAs Substrates. *Appl. Phys. Lett.* **2020**, *117*, No. 021102.

(8) Ludewig, P.; Reinhard, S.; Jandieri, K.; Wegele, T.; Beyer, A.; Tapfer, L.; Volz, K.; Stolz, W. MOVPE Growth Studies of Ga(NAsP)/(BGa)(AsP) Multi Quantum Well Heterostructures (MQWH) for the Monolithic Integration of Laser Structures on (001) Si-Substrates. *J. Cryst. Growth* **2016**, *438*, 63−69.

(9) Ludewig, P.; Diederich, M.; Jandieri, K.; Stolz, W. Growth of high N containing GaNAs/GaP/BGaAsP multi quantum well structures on Si (001) substrates. *J. Cryst. Growth* **2017**, *467*, 61−64.

(10) Hart, G. L. W.; Zunger, A. Electronic structure of BAs and boride III-V alloys. *Phys. Rev. B: Condens. Matter Mater. Phys.* **2000**, *62*, 13522−13537.

(11) Tischler, M. A.; Mooney, P. M.; Parker, B. D.; Cardone, F.; Goorsky, M. S. Metalorganic vapor phase epitaxy and characterization of boron-doped (Al,Ga)As. *J. Appl. Phys.* **1992**, *71*, 984−992.

(12) Gupta, V. K.; Koch, M. W.; Watkins, N. J.; Gao, Y.; Wicks, G. W. Molecular beam epitaxial growth of BGaAs ternary compounds. *J. Electron. Mater.* **2000**, *29*, 1387−1391.

(13) Groenert, M.; Averbeck, R.; Hösler, W.; Schuster, M.; Riechert, H. Optimized growth of BGaAs by molecular beam epitaxy. *J. Cryst. Growth* **2004**, *264*, 123−127.

(14) Ptak, A.; Beaton, D.; Mascarenhas, A. Growth of BGaAs by molecular-beam epitaxy and the effects of a bismuth surfactant. *J. Cryst. Growth* **2012**, *351*, 122−125.

(15) Geisz, J.; Friedman, D.; Kurtz, S.; Olson, J.; Swartzlander, A.; Reedy, R.; Norman, A. Epitaxial growth of BGaAs and BGaInAs by MOCVD. *J. Cryst. Growth* **2001**, *225*, 372−376.

(16) Dumont, H.; Rutzinger, D.; Vincent, C.; Dazord, J.; Monteil, Y.; Alexandre, F.; Gentner, J. L. Surface segregation of boron in BxGa1-xAs/GaAs epilayers studied by x-ray photoelectron spectroscopy and atomic force microscopy. *Appl. Phys. Lett.* **2003**, *82*, 1830−1832.

(17) Detz, H.; MacFarland, D.; Zederbauer, T.; Lancaster, S.; Andrews, A.; Schrenk, W.; Strasser, G. Growth rate dependence of boron incorporation into BxGa1-xAs layers. *J. Cryst. Growth* **2017**, *477*, 77−81.

(18) Hamila, R.; Saidi, F.; Rodriguez, P.; Auvray, L.; Monteil, Y.; Maaref, H. Growth temperature effects on boron incorporation and optical properties of BGaAs/GaAs grown by MOCVD. *J. Alloys Compd.* **2010**, *506*, 10−13.

(19) Geisz, J. F.; Friedman, D. J.; Kurtz, S.; Reedy, R. C.; Barber, G. Alternative boron precursors for BGaAs epitaxy. *J. Electron. Mater.* **2001**, *30*, 1387−1391.

(20) Duschanek, H.; Rogl, P. Critical assessment and thermodynamic calculation of the binary system boron-tungsten (B-W). *J. Phase Equilib.* **1995**, *16*, 150−161.

(21) Duzik, A.; Thomas, J. C.; Millunchick, J. M.; Lång, J.; Punkkinen, M.; Laukkanen, P. Surface structure of bismuth terminated GaAs surfaces grown with molecular beam epitaxy. *Surf. Sci.* **2012**, *606*, 1203−1207.

(22) Pillai, M. R.; Kim, S.-S.; Ho, S. T.; Barnett, S. A. Growth of InxGa1-xAs/GaAs heterostructures using Bi as a surfactant. *J. Vac. Sci. Technol., B: Microelectron. Nanometer Struct.–Process., Meas., Phenom.* **2000**, *18*, 1232−1236.

(23) Van Hove, J. M.; Cohen, P. I. Reflection High Energy Electron Diffraction Measurement of Surface Diffusion during the Growth of Gallium Arsenide by MBE. *J. Cryst. Growth* **1987**, *81*, 13−18.

(24) Neave, J. H.; Dobson, P. J.; Joyce, B. A.; Zhang, J. Reflection high-energy electron diffraction oscillations from vicinal surfaces—a new approach to surface diffusion measurements. *Appl. Phys. Lett.* **1985**, *47*, 100−102.

(25) Copel, M.; Reuter, M. C.; Kaxiras, E.; Tromp, R. M. Surfactants in Epitaxial Growth. *Phys. Rev. Lett.* **1989**, *63*, 632−635.

(26) Massies, J.; Grandjean, N.; Etgens, V. H. Surfactant Mediated Epitaxial Growth of InxGa1-xAs on GaAs (001). *Appl. Phys. Lett.* **1992**, *61*, 99−101.

(27) Tournié, E.; Ploog, K. H. Surfactant Mediated Molecular Beam Epitaxy of Strained Layer Semiconductor Heterostructures. *Thin Solid Films* **1993**, *231*, 43−60.

(28) Massies, J.; Grandjean, N. Surfactant Effect on the Surface Diffusion Length in Epitaxial Growth. *Phys. Rev. B: Condens. Matter Mater. Phys.* **1993**, *48*, 8502−8505.

(29) Tournié, E.; Grandjean, N.; Trampert, A.; Massies, J.; Ploog, K. H. Surfactantmediated Molecular-Beam Epitaxy of III-V Strained-Layer Heterostructures. *J. Cryst. Growth* **1995**, *150*, 460−466.
(30) Lu, X.; Beaton, D. A.; Lewis, R. B.; Tiedje, T.; Whitwick, M. B. Effect of Molecular Beam Epitaxy Growth Conditions on the Bi Content of GaAs1-xBix. *Appl. Phys. Lett.* **2008**, *92*, No. 192110.
(31) Pillai, M. R.; Kim, S.-S.; Ho, S. T.; Barnett, S. A. Growth of InxGa1-xAs/GaAs Heterostructures Using Bi as a Surfactant. *J. Vac. Sci. Technol., B: Microelectron. Nanometer Struct.–Process., Meas., Phenom.* **2000**, *18*, 1232−1236.
(32) Tixier, S.; Adamcyk, M.; Young, E. C.; Schmid, J. H.; Tiedje, T. Surfactant Enhanced Growth of GaNAs and InGaNAs Using Bismuth. *J. Cryst. Growth* **2003**, *251*, 449−454.
(33) Young, E. C.; Tixier, S.; Tiedje, T. Bismuth Surfactant Growth of the Dilute Nitride GaNxAs1-X. *J. Cryst. Growth* **2005**, *279*, 316−320.
(34) Williams, F. V.; Ruehrwein, R. A. The Preparation and Properties of Boron Phosphides and Arsenides. *J. Am. Chem. Soc.* **1960**, *82*, 1330−1332.
(35) Chu, T. L.; Hyslop, A. E. Crystal Growth and Properties of Boron Monoarsenide. *J. Appl. Phys.* **1972**, *43*, 276−279.
(36) Lindsay, A.; O'Reilly, E. P. Theory of Electronic Structure of BGaAs and Related Alloys. *Phys. Status Solidi C* **2008**, *5*, 454−459.
(37) Hamila, R.; Saidi, F.; Fouzri, A.; Auvray, L.; Monteil, Y.; Maaref, H. Clustering Effects in Optical Properties of BGaAs/GaAs Epilayers. *J. Lumin.* **2009**, *129*, 1010−1014.
(38) Matthews, J. W.; Blakeslee, A. E. Defects in Epitaxial Multilayers. *J. Cryst. Growth* **1974**, *27*, 118−125.
(39) Salviati, G.; Ferrari, C.; Lazzarini, L.; Nasi, L.; Drigo, A. V.; Berti, M.; Salvador, D. D.; Natali, M.; Mazzer, M. Structural Characterization of InGaAs/InP Heterostructures Grown under Compressive and Tensile Stress. *Appl. Surf. Sci.* **2002**, *188*, 36−48.
(40) Ayers, J. E.; Kujofsa, T.; Rago, P.; Raphael, J. *Heteroepitaxy of Semiconductors*; CRC Press, 2016; pp 192−194.
(41) Svensson, S. P.; Hier, H.; Sarney, W. L.; Donetsky, D.; Wang, D.; Belenky, G. Molecular Beam Epitaxy Control and Photoluminescence Properties of InAsBi. *J. Vac. Sci. Technol., B: Nanotechnol. Microelectron.: Mater., Process., Meas., Phenom.* **2012**, *30*, No. 02B109.
(42) Daoud, S.; Bioud, N.; Bouarissa, N. Structural Phase Transition, Elastic and Thermal Properties of Boron Arsenide: Pressure-Induced Effects. *Mater. Sci. Semicond. Process.* **2015**, *31*, 124−130.

https://doi.org/10.1021/acs.cgd.1c00291
Cryst. Growth Des. XXXX, XXX, XXX−XXX